Palaeogeography, Palaeoclimatology, Palaeoecology 485 (2017) 504–516

Contents lists available at ScienceDirect

Palaeogeography, Palaeoclimatology, Palaeoecology

journal homepage: www.elsevier.com/locate/palaeo

Sea-level changes and carbonate platform evolution of the Xisha Islands (South China Sea) since the Early Miocene

Lei Shao [a], Yuchi Cui [a,*], Peijun Qiao [a], Daojun Zhang [b], Xinyu Liu [b], Chuanlun Zhang [a]

[a] State Key Laboratory of Marine Geology, Tongji University, Shanghai 200092, China
[b] Zhanjiang Branch of China National Offshore Oil Corporation, Guangzhou 524057, China

ARTICLE INFO

Article history:
Received 16 March 2017
Received in revised form 4 July 2017
Accepted 8 July 2017
Available online 12 July 2017

Keywords:
BIT
Elemental geochemistry
Coral reef carbonates
Miocene–Pleistocene

ABSTRACT

Analyses of the biogeochemical branched and isoprenoid tetraether (BIT) index and elemental geochemistry from Well XK1 provide insight into the development of the Xisha Islands carbonate platform in the South China Sea (SCS) since the Early Miocene. BIT is the ratio of branched glycerol dialkyl glycerol tetraethers (bGDGTs) to isoprenoid glycerol dialkyl glycerol tetraethers (iGDGTs), which are derived from meteoric and marine environments respectively. BIT serves as a novel proxy for tracking sea-level changes.

The BIT curve of Well XK1 is characterized by "low–high–low–high" alternating stages, indicating the superposition of sea-level changes on carbonate platform evolution in the SCS. Following the rapid expansion of the SCS in the early stages of the Early Miocene, biogenic reefs began to form, and BIT oscillated intensely. The SCS started to regress after its initial expansion during the Middle Miocene, at which time global sea level was also falling significantly. The combination of both tectonic activity and eustatic variation has resulted in the deposition of strata with reef-beach facies, which are characterized by high BIT values. Relative sea level reached its lowest point in the late stages of the Middle Miocene (~11.6 Ma). Subsequent sea-level rise between the Late Miocene and Pliocene induced a negative shift in BIT, and lagoonal facies formed under optimal warm marine conditions. Periodic exposure caused the reefs of the Xisha Islands to suffer from erosion during the Pleistocene, which is consistent with a second elevation in the BIT index. However, modern trends show increasing regional water depths again. Major and trace element curves (Na, Si, P, B, Ga, Mo, Zn), as well as the associated ratios (Na_2O/K_2O, Na_2O/SiO_2, B/Ga, Ti/Sr, Zr/Sr, Al/Sr, Th/U), accurately record sea-level variations. Several significant discontinuities correlate with sea-level shifts, and provide important details about the geomorphology, sedimentation patterns, and diagenesis types on the SCS carbonate platform. The agreement between organic and inorganic geochemical data demonstrates that our reconstructions of SCS sea-level changes and modes of carbonate platform development are robust.

Our findings also demonstrate that carbonate evolution in the Xisha Islands was shaped by relative sea-level changes, implying that sea level fluctuations in the SCS were controlled by global eustatic factors in addition to regional tectonic subsidence.

1. Introduction

Carbonate platforms, composed of high volumes of biogenic sediment, are widespread in tropical and subtropical areas, especially in the clear shallow waters of Southeast Asia, such as the South China Sea (SCS) (Umbgrove, 1947; Longman and Siemers, 1992; Bachtel et al., 2004). Bathymetrically, carbonate buildups in the SCS form on basement plateaus, created by faulting on the southern margin during the Eocene/Early Oligocene (Fulthorpe and Schlanger, 1989; Sales et al., 1997; Moss and Chambers, 1999; Fournier et al., 2004, 2005). These blocks largely formed prior to those generated on the northern margin (Erlich et al., 1990; Erlich et al., 1993; Wilson, 2002), and western carbonates display younger age characteristics than those in the eastern SCS (Holloway, 1982; Wilson, 2002).

During the past few years, interpretations of geological and geophysical evidence have indicated that the interactions of global eustasy, geotectonics, and climatic variation exert a substantial control on reef evolution. These factors combine to influence the origin, proliferation, and demise of reef environments, and control their sedimentation processes (Fulthorpe and Schlanger, 1989; Wilson, 2002; Wu et al., 2014; Arosi and Wilson, 2015; Paumard et al., 2016; Shao et al., 2017). Global sea level is considered to be one of the most important factors controlling coral reef platform formation (Broecker et al., 1968; Edinger et al., 2007). Eustatic sea-level changes—global ocean volume fluctuations—are closely

* Corresponding author at: State Key Laboratory of Marine Geology, Tongji University, 1239 Siping Road, Shanghai 200092, China.
E-mail address: cuiyuchi@tongji.edu.cn (Y. Cui).

http://dx.doi.org/10.1016/j.palaeo.2017.07.006
0031-0182/

related to the cyclic advance and retreat of high-latitude ice sheets (Lambeck and Chappell, 2001). Regional variations, such as tectonic deformation and the gravitational responses of the earth-ocean system to the ice-water load changes, also have to be considered (Masao and Kurt, 1987; Kaufmann and Lambeck, 2000; Johnston, 2007). Representative carbonate materials, including deep-water sediments and submerged speleothems, have yielded relatively high-resolution sea-level curves from their marine oxygen isotope signals. Age models based on radiocarbon dating or U/Th series chronology, with iterated deconvolution, approximation solutions, and a final probabilistically assessment for model predictions, have been applied (Chappell, 1983; Lisiecki and Raymo, 2005). In many cases, regional tectonic activity may also play a central part in preventing carbonate sediments from being buried by siliciclastic sediment fluxes, by shaping the hinterland topography and river drainage systems (Hutchison, 2004; Dan, 2005). Lastly, temperature, salinity, nutrient supply, and certain bottom currents are important factors that shape reef structures (Lüdmann et al., 2013).

Coral reef carbonates typically develop in environments favorable for long-term geologic preservation. However, falling sea level can expose shallow platforms and produce widespread unconformities, leading to gaps in the record (Purdy, 1974; Kendall and Schlager, 1981). For example, Meyers (1974) described freshwater cementation and karst development associated with the subaerial exposure of Mississippian limestones in New Mexico during a period of eustatic sea-level fall. Many researchers have focused on material dating back to the Quaternary, especially since the Last Glacial Maximum (LGM). Coastal plain boreholes in New Jersey and Delaware have been used to estimate late Cretaceous to Miocene sea-level changes using the backstripping method (Van et al., 2004). Additionally, geophysical data compilations have contributed to our understanding of sea level change. However, sea-level studies based on carbonates in the SCS region are still controversial; issues such as the distribution patterns of reefs, their evolutionary histories, and the factors controlling their development are debated in the literature (Lü et al., 2013; Steuer et al., 2013; Wu et al., 2014; Wu et al., 2016). Although carbonate terraces have been widely investigated, better chemical proxies directly reflecting biogenic carbonate production are required. New tools are also needed to solve the problem of scarce data points around disconformities.

In recent years, glycerol dialkyl glycerol tetraethers (GDGTs) have become a promising tool in paleoenvironmental studies (Schouten et al., 2002). The branched and isoprenoid tetraether (BIT) index is a proxy that quantifies the relative abundance of terrestrially derived tetraether lipids versus crenarchaeol, which reflects the relative contribution of organic soil matter in marine environments (Hopmans et al., 2004; Sinninghe Damsté et al., 2009). This index ranges from 0, which represents no branched GDGTs, to 1, which indicates no marine crenarchaeol (Hopmans et al., 2004). BIT remains relatively constant with increasing temperature (Huguet et al., 2008; Huguet et al., 2009), and increases with increasing organic matter maturity and with oxic sedimentary environments. Therefore, compaction processes during diagenesis may alter this index to a certain extent. Additionally, BIT does not contain an aeolian component (Schouten et al., 2013). As a result, previous studies have utilized BIT as supporting evidence for sea-level variation (Sluijs et al., 2008), one that is interpreted to vary along a transect from the estuary to the open sea. As this study shows that BIT differs in different sedimentary facies, this index might potentially prove a useful supplementary index to reconstruct a long-term sea-level curve in our marine carbonate samples from the unique location of the Xisha Islands.

Generally, the elemental geochemistry of marine sediments includes both biogenic materials (e.g., carbonates or organic carbon) and authigenic elements (e.g., Mn and scavenged Al) (Elderfield, 1990; Mangini et al., 1990; Murray and Leinen, 1993). In recent years, elemental tracers derived from coral reef carbonates have been employed to reconstruct marine thermal conditions, to investigate the chemical composition of terrestrial inputs in seawater, and to detect biologic activity (Beck et al., 1992; Fallon et al., 2002; Wyndham et al., 2004). Nutrient-type trace elements incorporated into the calcium carbonate matrix have been used to evaluate sea-level fluctuations, paleoclimatic change, and primary productivity. Some trace elements, such as P, Ba, and S, as well as heavy metals including Cu, Zn, Cd, are involved in the biological cycling of micro- or nano-nutrients (Stüben et al., 2002). In other cases, major, trace or rare earth elements (REE) reflect the terrigenous sediment supply. For example, Zr, Ti and Al in marine sediments are usually correlated with detrital influx, though they can still be indicative of depth variations in certain settings (Xi et al., 2005). In previous studies, elemental proxies have shown great potential for reconstructing sea-level variations, but most of the research employing this method focuses on short-term variations.

Given the lack of in-depth research and the need for better indices on the ecology of SCS reefs, more detailed evidence is needed to shed light on the sea-level fluctuations and processes of carbonate platform development in this unique area. The goals of this study are as follows:

1) Test the utility of BIT, a novel but promising biogeochemical tool, as a proxy for changes in sea level, documenting both its advantages and weaknesses; 2) use traditional inorganic geochemical methods as an auxiliary dataset to examine the robustness of BIT; 3) apply this suite of geochemical methodologies to whole-core samples for the first time, to establish a long-term sea-level variation curve for the SCS since the Early Miocene; 4) determine how coral reef carbonate platforms evolved in the Xisha Islands; and 5) develop a better understanding of how the complex factors controlling reef development interacted with each other, and combined to influence the framework of reefs.

2. Geologic setting

The SCS is the largest marginal sea in East Asia, stretching between the equator and the Tropic of Cancer. It is surrounded by the South China Block, Taiwan Island, the Luzon Arc, Palawan, Borneo, and the Indo-China Peninsula. The SCS originally formed as a result of rapid seafloor spreading during the Cenozoic (Taylor and Hayes, 1983; Clift and Lin, 2001; Barckhausen and Roeser, 2004). Due to its unique position, the SCS has proven to be one of the most significant regions for carbonate platform development since the Miocene.

The Xisha Islands (17°07′–15°43′N, 111°11′–112°54′E) are situated on an elevated submarine plateau, which rises from the lower slope southeast of Hainan Island (Fig. 1). The islands are surrounded by marine waters that reach depths of over 1000 m (Xi et al., 2005; Ma et al., 2011). Scientific and commercial drilling programs conducted in the 1970s and 1980s provided extensive data on the biostratigraphy, lithology, sedimentology, paleomagnetism, and seismology of the islands, as well as information on the morphology of biota. Specific wells such as Xiyong-1, Xiyong-2, Xichen-1, Xishi-1, and XK1 record regional paleooceanographic events, in addition to global climatic and ecological changes (Liu et al., 1997; Shi et al., 2002). However, these early boreholes were limited in their utility due to incomplete core recovery and a lack of basement drilling, with the exception of Well XK1 on Shidao Island (16°50′41″N, 112°20′50″E; altitude: +1.5 m, bottom: −1268.2 m, average recovery: 70%). Our data are the result of numerous technological developments since the original drilling programs, and have the potential to reveal the connections between sea-level changes and carbonate platform evolution in the SCS.

3. Materials and methods

Well XK1 was densely sampled, to characterize lithology, microtexture, and to identify sedimentary facies. This qualitative overview of the sediments provides support to the BIT and elemental geochemistry results. Additional dating and stratigraphic correlations were made based on foraminiferal data.

A total of 2647 samples were analyzed. A total of 187 samples, collected at an interval of 0.5–1 m in the upper section and 5–8 m in the lower section, were analyzed for organic biomarkers at the State Key Laboratory of Marine Geology, Tongji University.

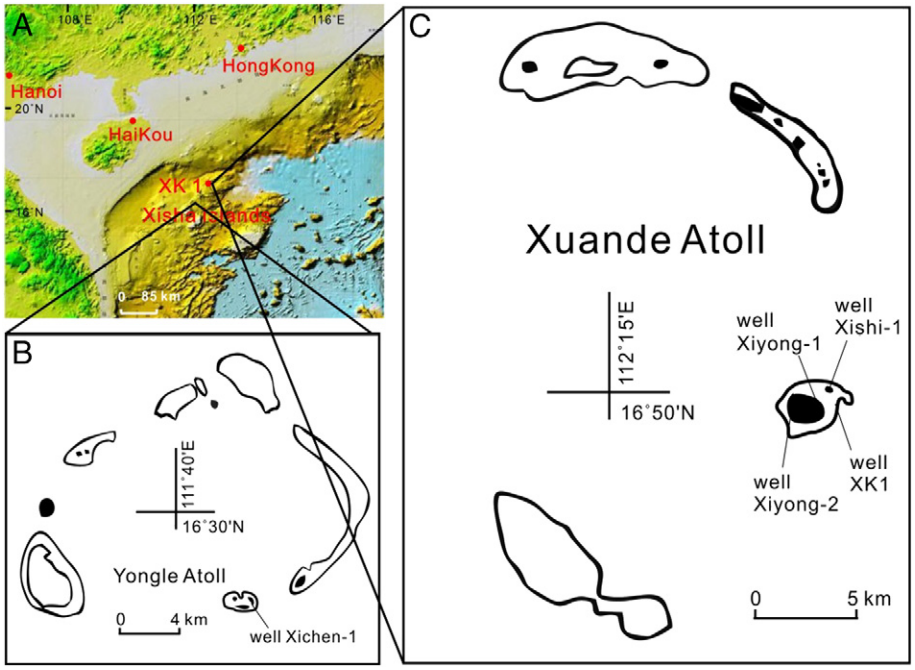

Fig. 1. Locations of Xisha Islands with positions of wells.

Isoprenoid GDGT molecules (iGDGTs) with 0 to 4 cyclopentane moieties are mainly synthesized by marine Thaumarchaeota (iGDGT I–IV mass to charge ratios (*m/z*) 1302, 1300, 1298, 1296, Fig. S1.A) (Gentsch and Schützbosbach, 2000). Other iGDGTs identified as crenarchaeol V (*m/z*: 1292) and its isomer V′ (*m/z*: 1292′) contain one cyclohexane plus another four cyclopentane moieties (Sinninghe Damsté et al., 2002; Schouten et al., 2008). Branched GDGTs (bGDGTs) contain methyl-substituted C_{28}n-alkyl side chains, in combination with the distinct 1,2-di-*O*-alkyl-*sn*-glycerol stereo configuration instead of C_{40} isoprenoidal alkyl chains (Sinninghe Damsté et al., 2000, 2002). Basically, bGDGTs without any cyclopentyl moieties are in higher abundance (VIa, VIIa, VIIIa with *m/z* of 1050, 1036 and 1022, Fig. S1.A) while ring-containing GDGTs exist in lower concentrations (VIb, VIc, VIIb, VIIc, VIIIb, VIIIc with *m/z* of 1048, 1046, 1034, 1032, 1020 and 1018, Fig. S1.A) (Weijers et al., 2006). These compounds are probably biosynthesized by bacteria, and are ubiquitous in global terrestrial and aquatic environments. However, studies have indicated that bGDGTs are preferentially accumulated in terrestrial environments such as estuaries (Lydie et al., 2006; Walsh et al., 2008). Crenarchaeol is most abundantly generated in deeper aquatic settings, but it can also be detected at extremely low concentrations in peats and soils (Hopmans et al., 2004). BIT is defined as follows:

$$\mathrm{BIT} = \mathrm{Via} + \mathrm{VIIa} + \mathrm{VIIIa}/\mathrm{Via} + \mathrm{VIIa} + \mathrm{VIIIa} + \mathrm{V} \quad (1)$$

The numerals in the function refer to the corresponding GDGTs shown in Fig. S1. Panel A.

Frozen dried sediments (ca. 20 g), as well as a standard material (C_{46}-GDGT), were ultrasonically extracted with dichloromethane (DCM) and methanol (×6; 3:1, v/v). After sonication was completed, samples were centrifuged (4 min, 3500 rpm), and the supernatant was dried under a nitrogen gas atmosphere (at a water bath temperature no higher than 40 °C). The total lipid extraction was then ultrasonically dissolved in hexane: isopropanol (99:1, v/v) and filtered through 0.45 μm, 13-mm diameter PTFE filters prior to injection. The extracts were separated by Al_2O_3 column chromatography using hexane/DCM (9:1) and DCM/methanol (1:1) to yield the apolar and polar fractions, respectively. The polar fractions were analyzed by high-performance liquid chromatography/atmospheric pressure chemical ionization mass spectrometry (Agilent 6460 Triple Quad HPLC/APCI-MS).

The procedure for HPLC/MS analyses of the purified extracts was modified from Hopmans et al. (2000). Compounds were separated using an Alltech Prevail Cyano column (150 mm × 2.1 mm, 3 μm; Alltech, USA), maintained at 30 °C; injection volume was 10 μl. Tetraethers were eluted isocratically with 99% hexane and 1% isopropanol for 5 min, followed by a linear gradient to 1.8% isopropanol over a 45 min period using a flow rate of 0.2 ml/min. After each analysis, the column was cleaned by back-flushing hexane/isopropanol (99:1; v/v) at 0.2 ml/min for 10 min. Conditions for APCI-MS were as follows: nebulizer pressure 60 psi, vaporizer temperature 400 °C, drying gas (N_2) flow 6 l/min, temperature 200 °C, capillary voltage −3 kV and corona 5 μA (−3.2 kV). Ion mass scanning was performed using a selected ion-monitoring (SIM) mode in order to increase sensitivity and reproducibility. GDGTs were detected by mass scanning with a range covering *m/z* of 1302, 1300, 1298, 1296, 1292, 1050, 1048, 1046, 1036, 1034, 1032, 1022, 1020 and 1018. The relative GDGT distribution was measured by integrating the areas of relevant peaks on the chromatogram and comparing them with the peak area of the internal standard (Huguet et al., 2006).

The remaining 2460 core samples were analyzed for their elemental geochemistry at the State Key Laboratory of Marine Geology, Tongji University, using an inductively coupled plasma atomic emission spectrometer (ICP-AES) and inductively coupled plasma emission mass spectrometer (ICP-MS) for major (1245 samples) and trace (1215 samples) element analysis, respectively. Samples were corrected using an external standard for adjustment. Prior to analysis, samples were completely dissolved in a mixture of HF and HNO_3. HF was used on our carbonate sediments, as biogenic or terrestrial-source silica may be a useful index. Each sample was measured 6 times, with 1 ppb of Ru or In as an internal standard. Precision was better than 2% for all analyzed elements, which was determined by international certified materials, namely International Standards AGV-2, BCR-2, and BHVO-2 and Chinese National Standard GBW07120, provided by the Institute of Geophysical and Geochemical Exploration, China. Analyses were repeated to increase precision.

4. Data quality assessment

Marine carbonates preserved in the geological record can be altered to a greater or lesser degree by diagenesis. Numerous studies have

indicated that the elemental concentrations of Mn and Sr are important indicators for evaluating the degree of diagenetic alteration, including the effects of meteoric diagenesis and dolomitization (Kaufman and Knoll, 1995). Generally, Sr tends to be expelled out of marine carbonates during diagenesis, while Mn is preferentially incorporated when carbonates are exposed to meteoric fluids. Higher Mn/Sr ratios are attributed to the addition of Mn or the removal of Sr through the meteoric diagenesis (Kaufman et al., 1993). Originally, Derry et al. (1992) and Kaufman et al. (1993) proposed that reliable Sr isotopic values are most likely to come from carbonates that show Mn/Sr ratios with an upper limit around 2–3. However, this parameter is not reliable across all conditions, as the Mn/Sr ratio can be easily altered while other geologically informative elements are not much affected. It has also been suggested that carbonates retain a reliable geochemical record if their Mn/Sr values are lower than 10 (Kaufman and Knoll, 1995). Another principal geochemical signal that is sensitive to diagenesis is the oxygen isotopic composition, which tends to decrease during isotopic exchange with meteoric or hydrothermal fluids. $\delta^{18}O$ values ranging from 0 to −5‰ are observed in the least altered limestones. Values less than −5‰ would represent a mild degree of alteration, while those below −10‰ are considered unacceptably altered. In our borehole samples, Mn/Sr values range between 0.0023 and 1.2711, with an average value of 0.078 (except for several higher data points collected close to the gneissic basement). Our $\delta^{18}O$ results range from −9.18‰ to +4.77‰, with an average of −3.50‰, all of which are above the lower limit of −10‰ (Fig. 2).

Correlation coefficients of the borehole bulk elements are shown in Table S1. Trace elements display an average correlation of −0.32 with CaO and 0.08 with MgO. The poor correlation of these trace elements with the major components indicates a relatively small degree of diagenetic alteration of trace elements. This indicates that the trace elements have excellent potential as proxies reflecting chemical changes in seawater.

Terrigenous components are also an important component of marine sediments, and require careful assessment. For our core materials, we investigated the abundance of terrigenous material and its effect on authigenic elements. Well XK1 has been isolated from the main continent since the formation of the Xisha Block during the early Cenozoic. Our samples are highly pure coral reef carbonates, with a high core recovery rate and CaO content over 50% in most sections. Therefore, terrestrial materials transported by fluvial plumes, such as mud, sands, or conglomerates will not be considered further in this study. Inorganic geochemical proxies are mostly related to variations in seawater composition, which reflect the relative strength of the marine and terrigenous fluxes within the oceanic system as a whole.

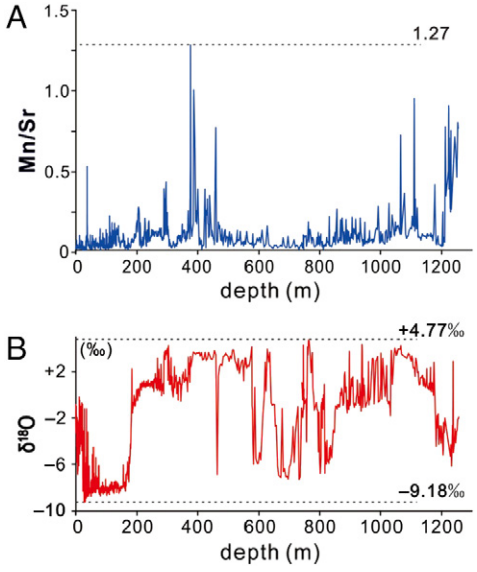

Fig. 2. (A) Mn/Sr curve and (B) $\delta^{18}O$ curve with depth variations in Well XK1. Dotted lines and numbers mark data ranges.

Based on observations of HPLC-MS base-peak chromatograms of both iGDGTs and bGDGTs (Fig. S1.B–F), we note that the detected GDGT components are high in concentration, displaying tight and distinct peak clusters. Several different groups of organic compounds were identified and quantified in our analysis. We also note that the abundance of bGDGTs is higher than that of iGDGTs. Increased diagenetic alteration and degradation may lead to a lower accumulation of GDGTs in deeper samples relative to surficial samples. Nevertheless, the majority of our samples yielded realistic results.

5. Results

5.1. Petrography and biostratigraphy

The uppermost section (20–0 m) of the core is composed of weakly cemented calcite bioclasts. The underlying section (160–20 m) consists of a set of moderately fragmented, light-colored yellowish-white reef limestones with light greyish-white interlayers dominated by corals and foraminifera (Fig. 3). The 280–160 m interval is mainly composed of light-colored, yellowish-white bioclastic limestones with greenish-grey reef and bioclastic limestone interlayers. Additionally, laminae enriched in dark organic matter are widely developed. This section is typically fragmented, and weakly dolomitized.

The 300–280 m section contains weakly to moderately fragmented reef limestones, some of which are dolomitized. The section (380–300 m) then becomes dominated by strongly fragmented, yellowish-white bioclastic limestones, which contain foraminifera and bivalves. Weak corrosion and algal laminae are discontinuously developed in the 376–373 m section.

Between 460 and 380 m, light yellowish-white bioclastic dolomites are strongly fragmented, and contain a lower abundance of bivalve molds. Further downwards (480–460 m), light greyish-white fragmented dolomites with abundant algal aggregates and laminae are developed. The section from 540 to 480 m is composed of light yellowish-white organic reef dolomites, which are moderately fragmented and contain corals, gastropods, and biogenic molds.

The interval from ~1100 to 540 m is dominated by light greyish to greyish-white bioclastic limestones, most of which are fine-grained and weakly cemented. Strong emersion, denudation, dissolution, and corrosion are widely developed in the middle (770–740 m) and lower (1069.44–1032.46) parts of this succession. Algal detritus or aggregates are sporadically distributed in certain layers (e.g. 640–620 m), and occur more frequently near the top (e.g. 577–565 m). Additionally, in intervals of 640–620 m and 580–540 m, greyish-white calcareous dolomites are found, some of which are moderately to strongly fractured.

The basal Cenozoic carbonate (1257–1100 m) in Well XK1 is composed of light-grey reef limestones, containing abundant fossils. It unconformably overlies Paleozoic or older gneissic basement. The 1119–1097.42 m and 1245.8–1228.92 m intervals are characterized by iron-rich erosional boundaries, and extensive dissolved pores and caves, while the 1218.92–1216.62 m section is a thick layer of greenish-grey to greyish-black silty pelite, rich in organic matter. Partially oolitic, light yellowish-white bioclastic limestones dominated by corals, foraminifera, and bivalves are found in the interval from 1220 to 1200 m.

5.2. BIT

The majority of BIT data ranges from 0.6 to 1 in the interval from 0 to 180 m (Figs. S1, 3), with only one anomalous value of 0.35 at 110.19 m, and several values of less than 0.5 in the surface samples. The interval from 180 to 560 m yielded lower BIT values, most of which are below 0.45, with a minimum of 0.05 and an approximate mean of 0.3. The curve then increases and plateaus through the 560–1032 m interval, with a maximum value of 0.9. A small group of data points from the

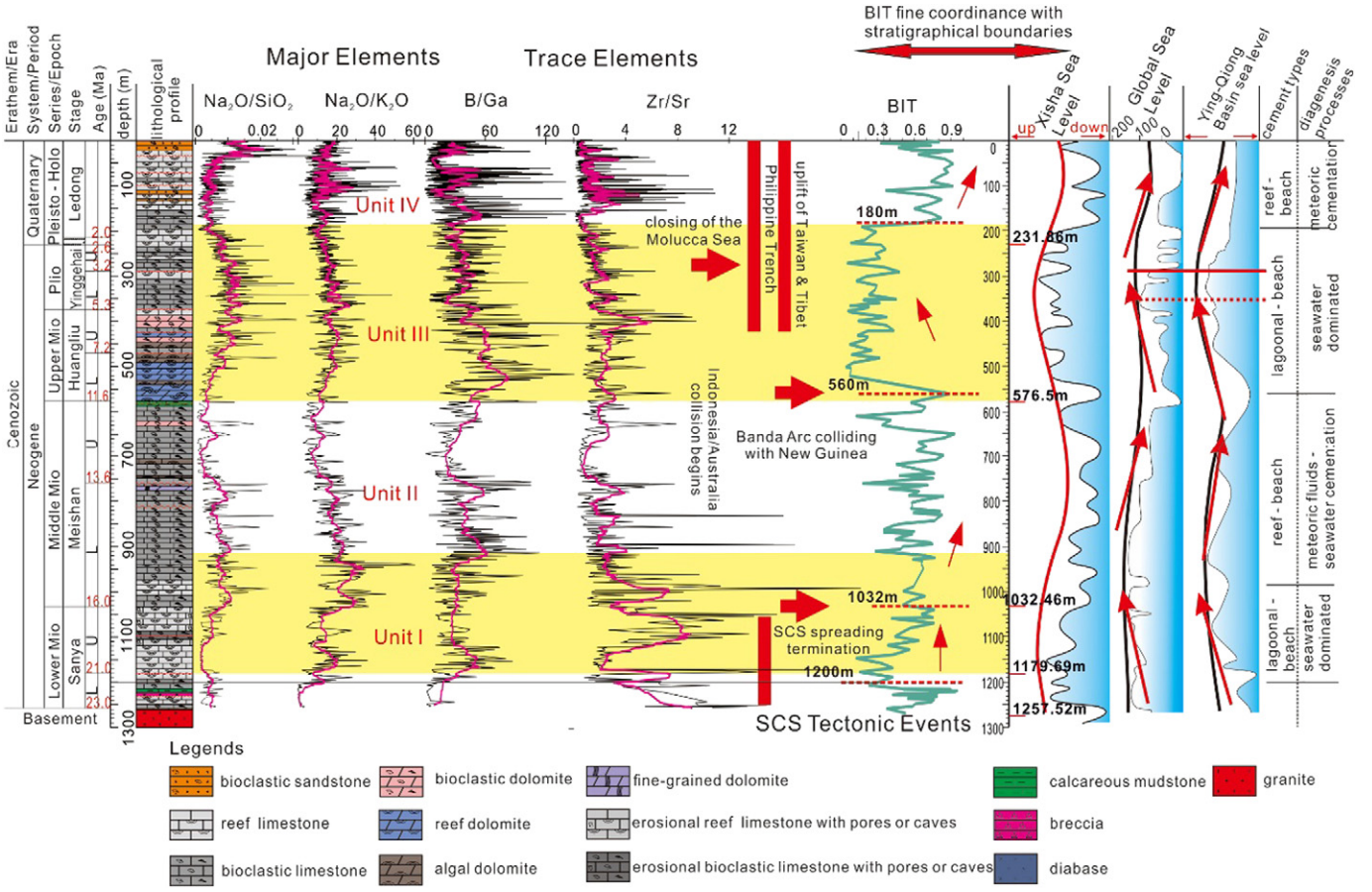

Fig. 3. Representative organic and inorganic proxies from Well XK1, with inferred sea-level variations. Inorganic indices include major element ratios of Na_2O/SiO_2 and Na_2O/K_2O, trace element ratios of B/Ga and Zr/Sr. Light purple lines represent a fifteen-point moving average. One organic index, the BIT curve, is also shown. Solid lines intersecting the right depth axis denote stratigraphic boundaries. Global and regional sea-levels are from Haq (1988) and Hao et al. (2000). "Xisha sea-level curve" is based on a combination of proxies.

610–630 m interval shows much lower values compared to the rest of the core. In addition, a few anomalies are observed within the section of fluctuating values between 650 m and 900 m. Despite these outliers, the majority of the data points show relatively high values. In the lowermost unit, which stretches from 1032 m down to the metamorphic basement, the curve shows a second overall decline. However, intense oscillations are observed in this interval, including some anomalously high values. In the short interval from 1032 to 1065 m, several values (0.75, 0.73, 0.74) appear to be incompatible. The BIT variations discussed above allow us to divide Well XK1 into four stages separated by significant inflection points, at 180 m, 560 m and 1032 m. These points closely align with the stratigraphic boundaries for the Pleistocene/Pliocene (216 m), Late Miocene/Middle Miocene (577 m), and Middle Miocene/Early Miocene (1032.46 m), according to Qiao et al. (2015) and references therein.

5.3. Elemental chemistry

5.3.1. Major elements

The abundances of major elements and elemental ratios in Well XK1 vary with depth, and most of the major elements show similar patterns of change (Figs. 3 and 4). For single elements, such as Na_2O, SiO_2, P_2O_5, and the related ratios, such as Na_2O/K_2O, Na_2O/SiO_2, the uppermost 200 m of the core displays a declining trend, with the exception of an extremely high P peak close to the surface. For SiO_2 and Na_2O/K_2O, a small group of higher values are observed in the 50–130 m interval. In comparison to the uppermost 200 m, the 200–550 m interval contains obvious peaks in most of the major element indicators. The maxima of Na_2O and SiO_2 are over 1.50% and 50% respectively, most P_2O_5 values fall between 0.05% and 0.08%, and the Na_2O/SiO_2 and Na_2O/K_2O ratios exceed 0.01 and 20, respectively. Overall, these indices tend to share common inflection points and follow similar first-order trends, though they differ substantially in detail. For example, abrupt increases in both $Na_2O/SiO_2$and Na_2O/K_2O values are observed at 341 m (0.04, 48.8). At approximately 300 m, SiO_2 displays a sharp decrease, which is mirrored by a corresponding decline in P_2O_5 at a similar depth.

In the interval from 550 to 950 m, element concentrations and ratios exhibit another substantial decrease (Na_2O: ~0–0.25%; SiO_2: ~40–45%; P_2O_5: ~0–0.05%; Na_2O/SiO_2: ~0–0.01; Na_2O/K_2O: ~5–15). Like the overlying succession, the upper and lower boundaries of different major element excursions do not occur at the same depth. From 750 to 950 m, oscillations are apparent in almost all of major elements and ratios, with increasing Na_2O, SiO_2 and P_2O_5 anomalies. Na_2O, K_2O, and P_2O_5 display higher values in the 750–800 m interval, while SiO_2 exhibits an opposing trend. Throughout the lowermost interval (950–1180 m), which overlies the metamorphic basement, most proxies (i.e., SiO_2, P_2O_5, and the ratio of Na_2O/K_2O) are quite high, while Na_2O and Na_2O/SiO_2 do not show any apparent increase. Differences between SiO_2 and P_2O_5 persist in this interval, with SiO_2 maintaining a smooth, elevated trend, while the other indices show an increase followed by a slight decrease. Element concentrations fluctuate greatly within the lowermost interval, which may be due to the vicinity of the basement, at around 1200 m. Nevertheless, the significant inflection points and seen in major elements and their ratios are in relatively good agreement with what our organic geochemical data (Figs. 3 and 4). However, the overall decreasing trend observed in SiO_2 concentrations beginning in the Early Miocene does present complications.

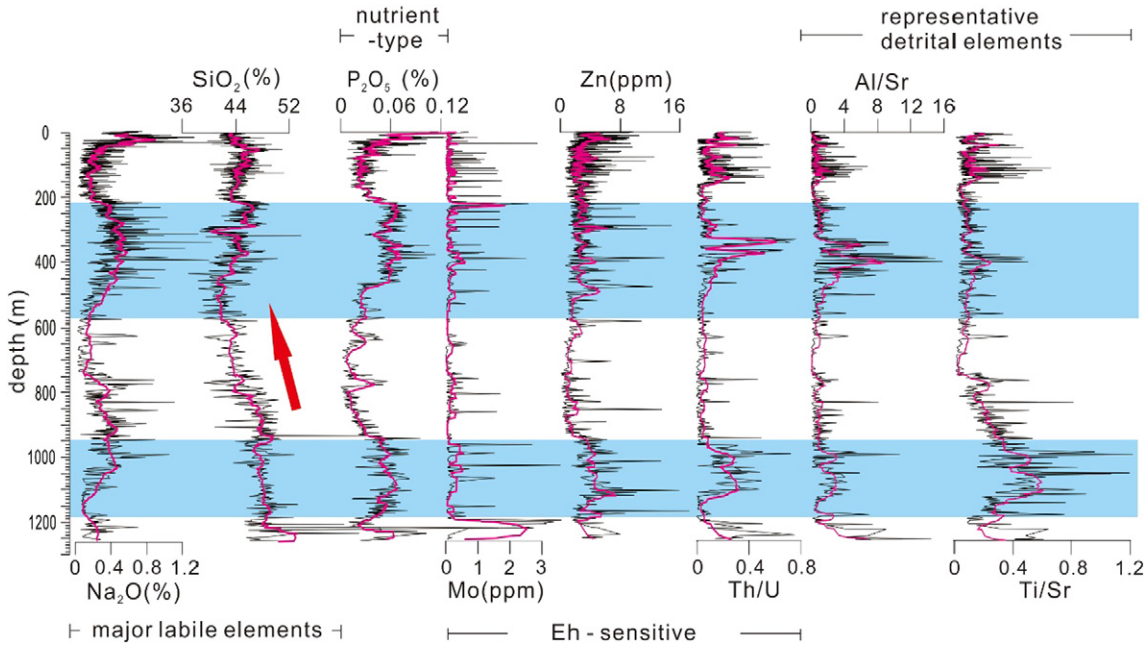

Fig. 4. Representative major element (Na_2O, SiO_2, P_2O_5), trace element (Mo, Zn), and element ratio (Th/U, Al/Sr, Ti/Sr) curves from Well XK1. Light purple lines show the fifteen-point moving average. The blue shaded areas divide these proxies into four major stages. Elements are separated into four groups based on their geochemical properties and behaviors.

5.3.2. Trace elements

Trace elements can be divided into three major clusters in this study: elements reflecting the detrital-biogenic ratio, elements sensitive to redox variations, and the remainder, which are potentially related to sea-level changes (Figs 3 and 4). Although intense oscillations are observed in trace element plots, the major variations in trace elements are similar to those observed in the major elements. For the majority of the 0–950 m succession, the variation in Mo is not as apparent as the other trace elements. Additionally, almost all proxies are marked by numerous high-value anomalies in the uppermost 150 m interval. Mo and B/Ga display smooth trends, while other trace elements typically display oscillating curves within the lowermost 1050–1150 m interval. The Ti/Sr ratio appears to lag behind the other curves, as it continues to decrease until 750 m, while others rapidly drop down to their minimum values at around 950 m.

6. Discussion

6.1. Implications of BIT measurements

Petrographic studies and thin section analyses indicate that the sediments of the Xisha reef platform can be described as an organic framework interbedded with bioclasts, including fossils of hermatypic organisms such as scleractinian corals and coralline algae, as well as other marine fossils such as foraminifera, ostracoda and calcareous nanoplankton. As the Xisha carbonate terraces are isolated from the main continent, there is very little terrestrial organic matter or clastic material transported by rivers in the sediments, and applying the conventional principles of BIT interpretation to our study would be misleading.

Given the samples' geographic location, the distinction between meteoric and marine sedimentation types is more appropriate than the typical division between terrestrial and oceanic environments. Moreover, the different groups of organisms that produce the GDGTs related to the BIT ratio will vary in abundance depending on the sedimentary environment. Since identification of sedimentary facies or microfacies is generally regarded as one of most reliable approaches for determining water depth (Flügel and Munnecke, 2004), we are attempting to extend the application of BIT as a proxy by relating it directly to observed sedimentological changes. We propose that this index reflects changes in the environment of organic matter formation, in either meteoric-exposed or fully marine settings, which is closely related to sea-level fluctuations. More detailed evidence will be provided in the following sections.

Lithological analysis reveals that strong exposure and leaching occurred in two intervals, from 0 to 180 m and 560 to 1032 m, indicative of shallow environments. Diagenetic alteration of the original reef limestones (composed of bioclasts and corals) is ubiquitous. Partial to complete dissolution of foraminifera, coralline algae, skeletal grains, and micritic substrate is observed in thin-sections. Furthermore, meniscus, dripstone, and drusy cement types are widespread, reflecting meteoric or meteoric-marine diagenetic environments (Fig. 5A, E, and F). In these two intervals, carbonate sediments may have experienced erosion to a greater or lesser degree when the Xisha reef platforms periodically emerged in response to major sea-level fluctuations. In contrast, in the 180–560 m and 1032–1200 m intervals, framework-supporting limestones are replaced by bioclasts, micrites, and coralline algae. Fibrous and bladed cements are widely distributed within inter- or intra-particle pores in these thin-sections (Fig. 5B, C, D, E, and F) These cements form thin fringes around grains, a morphology which only originates in marine sedimentary environments. These sedimentary facies and microfacies show that coral reefs thrived in a relatively optimal geologic setting, where exposure and corrosion were not common. Furthermore, carbonate terraces were also preserved during this interval.

The abundance of bacteria and marine Crenarchaeota in our samples, along with their GDGT index, changes in accordance with changing sedimentary environments. Organic input from freshwater or seawater sources reflects changes in sedimentary facies or microfacies, which were determined based on thin section and petrographic observations. When weakly acidic atmospheric conditions with abundant freshwater precipitation prevailed, reef platforms were severely eroded by leaching, resulting in a high volume of secondary porosity. As expected, these sections were characterized by high BIT values, representing a more rapid increase in bGDGTs compared to iGDGTs. After returning to a marine-dominated environment, BIT decreased, indicating a more rapid increase in iGDGTs. The synchronous shift in both BIT and sedimentary facies is

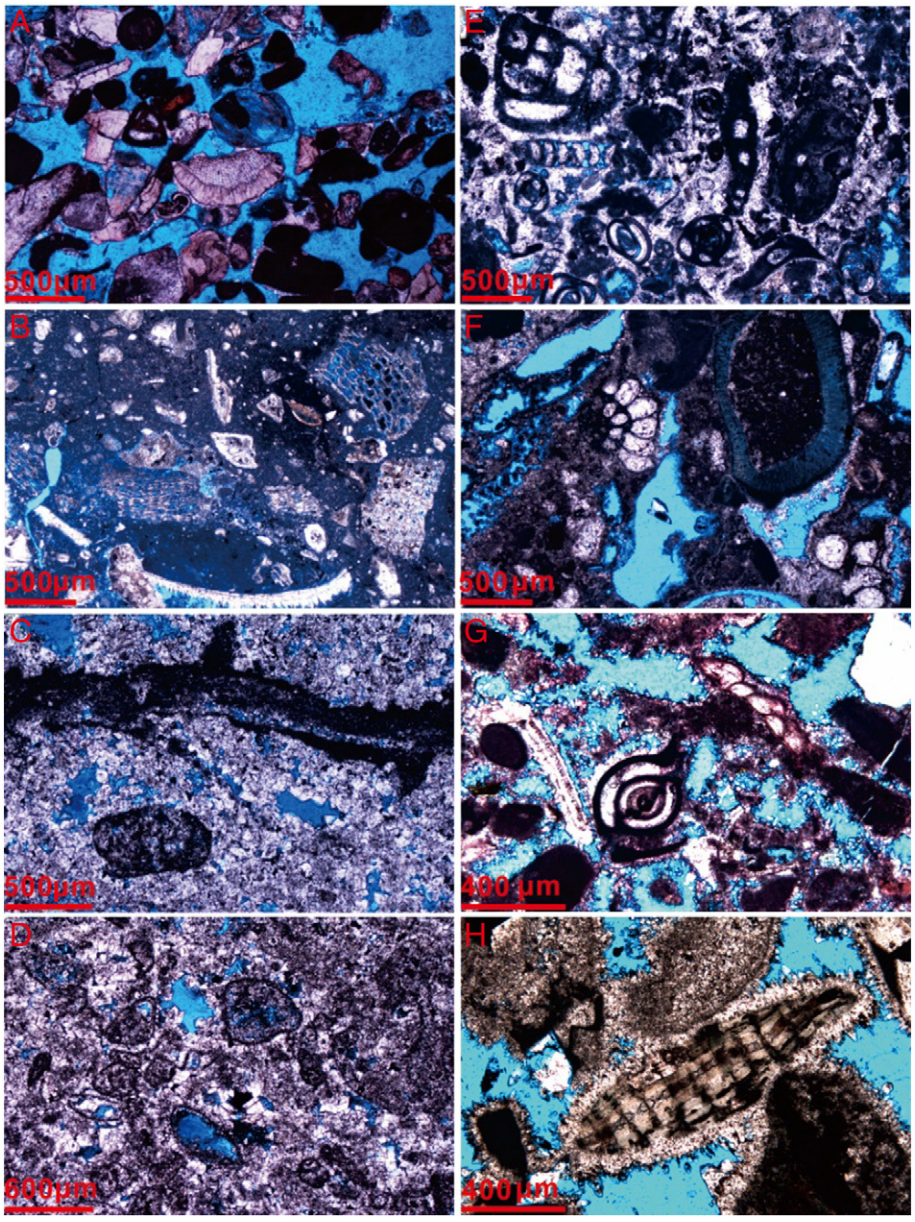

Fig. 5. Thin-sections at depths of (A) 7.96 m, (B) 251.48 m, (C) 483.91 m, (D) 546.36 m, (E) 747.67 m, (F) 862.19 m, (G) 1232.55 m, and (H) 1254.43 m, from Well XK1. (A), (E), and (F) show dripstone and meniscus cement types formed in a meteoric environment. (B), (G), and (H) show fibrous cement types, formed in seawater. (C) shows a blocky cement type, formed in a seawater-meteoric environment. (D) shows dripstone, granular, and blocky cement types, also from a meteoric-seawater environment.

consistent throughout our study. In this case, we can draw the preliminary conclusion that BIT variations in Well XK1 were regulated by changes between marine sedimentation and exposure during the evolution of the Xisha carbonate platform. As sea-level variation is generally regarded as one of the significant controls on sedimentary environments, BIT can be considered as a useful reflection of sea-level changes. Although experiments have not yet been carried out on modern reefs to demonstrate this correlation between BIT and water depth, we have demonstrated that this organic indicator has the potential to be an indirect proxy for water depth. Nevertheless, generating a reliable long-term sea-level curve requires robust data from other inorganic geochemical proxies, to supplement the results of organic analysis.

6.2. Elemental geochemistry

6.2.1. Nutrient types and biogenic elements

Nutrients play a significant role in carbonate production rate, bioerosion, and the formation and destruction of organic reef platforms (Wood, 1993). Phosphorus is an essential bio-limiting element required by all living organisms, is assumed to be supplied by terrestrial sediment flux, marine transgression, or the upwelling of cold, nutrient-rich waters (Kinsey and Davies, 1979; Bertrand et al., 2000; Saltzman, 2005). Under optimal light and temperature conditions, P availability can be the ultimate limiting factor for biological primary and secondary productivity via photosynthesis (Redfield, 1958). Studies have indicated that regional vertical circulation, eddies, and hydrothermal vents, as well as global circulation and even thermal-convective processes, can alter the concentrations of essential nutrient elements (Rougerie and Fagerstrom, 1994). The efficient recycling of nutrients will also be facilitated by reduced redox potential, with the recycling of dissolved P being enhanced under anaerobic conditions (Cappellen and Ingall, 1994; Filippelli and Delaney, 1996). Differences in nutrient levels can influence carbonate production by controlling the dominant reef biota and resulting carbonate types in autochthonous limestones, as well as by promoting the growth of non-carbonate producing planktonic organisms such as radiolarians and diatoms (Flügel and Munnecke, 2004).

Greater values of P_2O_5 are seen when sea level is rising (Figs. 3 and 4). The Xisha area was experiencing a highstand, with a more reducing marine environment, during the Early Miocene and the Late Miocene–Pliocene. Stronger upwelling and reworking of sediment may have provided abundant nutrients, derived from the decomposition of organic matter, to the sea surface. Marine organisms, including scleractinian corals, bryozoans, and algae absorbed these nutrients, resulting in the rapid development of carbonate platforms. During lowstand stages, such as the Middle to Late Miocene or Pleistocene, a weakening in upwelling and regional circulation led to a decreased nutrient flux from the deep sea. Coralline organisms grew at a slower rate, resulting in declining carbonate production. Due to rapid spreading processes in the SCS, the increase in P during the Early Miocene may also be related to remnant geothermal activity from volcanoes, which forced oceanic waters enriched in nutrients upward through the reef framework.

6.2.2. Labile element variations

The major elements sodium and potassium possess higher solubility in seawater than freshwater, due to their high chemical mobility. These elements also tend to adsorb more easily to clay minerals than to other sediments. Thin-section observations indicate that leaching and erosion are ubiquitous in intervals characterized by meteoric diagenesis, which is consistent with the expulsion of Na or K. Their concentrations vary in discrete stages, which might correspond to changes in sea level (Figs. 3 and 4). Throughout the Early Miocene, as well as during the Late Miocene–Pliocene, Na and K display high abundances reflecting their marine source. However, Na increases more rapidly relative to the alkaline-earth metals, possibly due to its smaller ionic radius and weaker energy of hydration. Na is often regarded as a possible proxy for paleosalinity, or the salinity of diagenetic solutions, in the tropical ocean. Previous studies have also indicated that Na is more soluble than K, especially in hypersaline marine environments, such as evaporate carbonate shorelines or lagoons (Lowenstein et al., 2001). Therefore, increasing trends in the Na_2O/K_2O ratio are likely to be indicative of a transition into a deeper, lower-energy depositional system. Conversely, when the Na_2O/K_2O ratio decreases, a shallower meteoric environment might have dominated. In our dataset, oscillations in Na in the 200–600 m interval may be linked to weak or moderate dolomitization, as a sharp increase in MgO to 20% is identified in the 290–310 m, 376–570 m, and 620–645 m intervals. Additionally, the average sedimentation rate for the Late Miocene is a low 32 m Myr^{-1}, with large forams sporadic or almost absent.

Similarly, boron is an unstable trace element, with a concentration that generally increases with salinity, which means that it has a higher concentration in seawater than freshwater. Conversely, gallium is less diagenetically mobile. Higher values of the B/Ga ratio reflect relatively more B dissolution, in a deeper and more saline environment. When sea level falls and sediments are exposed to meteoric diagenesis, gallium tends to be enriched. Therefore, variation in the B/Ga ratio might be governed to some extent by sea level fluctuations. However, this index seems to be sensitive to influence by terrestrial components after the Pleistocene, as initiation of the monsoon caused intense and frequent oscillations. This observation does not obviate the potential of B/Ga as a sea level proxy, but it does illustrate the way in which additional factors can govern elemental chemistry.

Like P, silicon is essential for organic framework synthesis. In the 200–800 m interval, variations in Si and P show similar patterns, which may reflect their role as bio-limiting elements. Under favorable conditions, when rising sea level generates a flooding surface, marine organisms can thrive by assimilating abundant silicon, reducing the Si content of the marine environment (Figs. 3 and 4). Additionally, silicon compounds occur in a much wider range of sediments, not only as biogenic opal and its related diagenetic products, but also glauconite, clay minerals, and detrital quartz from eolian sources (Jarvis, 2001). Therefore, we consider Si (from organic or inorganic sources) as a terrestrial-type element, in contrast with marine-type elements such as Na. Higher values of Na_2O/SiO_2 are seen during rises in sea level, as expected. As sea level falls, with considerable mortality of marine organisms, a large quantity of Si is released, leading to a decline in the Na_2O/SiO_2 ratio. Si declines slightly, from 50% to 40%, beginning in the Early Miocene. This may imply a decrease in volcanic activity, and an increasing predominance of biogenic silica over time.

6.2.3. Elemental ratios related to detrital material

Detrital elements (e.g., aluminum, zirconium, and titanium), preferentially accumulate in clay sediments and are generally not affected by biogenic or diagenetic processes (Cantalejo and Pickering, 2014). It has been suggested that Al is one of the best proxies for tracing terrigenous material in deep sea sediments (Schneider et al., 1997). Although some previous studies (e.g., Murray and Leinen, 1993) have suggested that excess Al will be scavenged by organic compounds in high-productivity zones, such a contribution of biogenic Al is likely to be negligible. Strontium is a biologically mediated element in the ocean system, and the mass flux of Sr to the ocean floor is primarily controlled by surface productivity (Schmitz, 1987). For coral reef carbonates, Sr tends to display a strong relationship with calcium, since Sr usually substitutes calcium in the calcite lattice. Additionally, Sr of terrestrial origin can be easily mobilized and incorporated into clay sediments transported by rivers and river plumes (Cantalejo and Pickering, 2014). However, the poor correlation ($R = 0.04$; $n = 1216$) between Al and Sr indicates that Sr in Well XK1 sediments mainly originates from biogenic sources. Moreover, the modest correlation between Al_2O_3 and TiO_2 demonstrates that both are mainly of lithogenic origin.

In our inorganic geochemical analysis, examining specific elemental ratios may enhance our understanding of sedimentary facies and sea-level changes, as these proxies commonly combine one detrital component enriched in clay minerals and an authigenic component generated in the marine environment. In the specific case of Well XK1, enrichment of "terrestrial-representative" elements is not always linked to provenance. Instead, due to the location of Well XK1, detrital elements are enriched in lagoonal facies during increases in sea level. Additionally, detrital component ratios, such as Al/Ti and Zr/Ti, remain stable throughout the whole carbonate sequence, precluding the possibility that the detrital matter was transported into our studying area by riverine plumes. When a lagoonal sedimentary environment was prevalent, detrital elements in seawater tended to stimulate the growth of plankton and fast-growing soft algae. The growth of corals was limited, possibly due to the reduction of water transparency and biological erosion, though biogenic Sr would also have accumulated in organic frameworks. Conversely, during periods of sea-level retreat, terrigenous elements were severely depleted, far in excess of the correlative decline in Sr.

6.2.4. Redox-sensitive elements

To some degree, marine redox conditions are influenced by sea-level variations. In closed or semi-closed oceanic basins, such as the Black Sea and the Sea of Japan, freshwater sedimentary environments shift into a more reducing mode during rises in sea level (Degens and Ross, 1974; Nakajima et al., 1996). Redox conditions have a critical influence on the oxidation state and solubility of certain elements, some of which actively participate in marine biological cycling (Pattan and Pearce, 2009); the evolution and extinction of living organisms can be dramatically influenced by redox conditions. Despite their extremely low concentrations, redox-sensitive elements can still be detected in our samples. Due to their preservation of seawater signatures, they can be used as high-resolution tracers to explore the history of the sedimentary environment.

Thorium, which is typically interpreted as a record of detrital input, is independent of source and grain size. Uranium typically occurs as U^{6+} under oxic conditions, and binds to carbonate ions (Langmuir, 1978; Taylor and McLennan, 1995). Under reducing conditions, it is usually enriched in a less stable form of U^{4+} (Wignall and Twitchett, 1996). The poor correlation of Th and U concentrations ($R = 0.33$; $n = 1216$) implies little influence from an extrinsic input. Consequently, Th/U can reflect regional redox conditions, and can serve as a proxy for

paleoenvironment reconstruction. As a micronutrient, the heavy trace metal Zn is known to be involved in certain biological processes, and generally reflects either high planktonic productivity or a detrital influx (Knauer and Martin, 1983; Stüben et al., 2002). Mo is also enriched in reducing depositional environments (Jacobs et al., 1987; Francois, 1988). Dean et al. (1999) confirmed that Mo content in the Cariaco Basin has increased over the past 24 kyr, during an interval of elevated primary productivity. As a nutrient-type element, Mo can also be absorbed by organic matter, and accumulate in sediments bound to carbonaceous materials.

During the lowstand phase, with a predominance of freshwater in diagenetic environments, Mo and Zn show low concentrations. The sedimentary setting becomes more oxidized and exposed, impeding the enrichment of redox sensitive elements. When sea level rises, and sediments accumulate in a setting with greater water depth, these elements become more enriched in the relatively reducing system. Similarly, the significant inflection points in redox conditions are almost identical to the boundaries delineated by organic and other elemental indices. Additionally, in reducing systems with greater water depth, Th tends to be absorbed by algae in higher concentrations, while U is less likely to bind with carbonate ions, leading to higher values of Th/U in lagoonal sediments. Mo content could potentially have been diluted by other terrestrial or shallow-water components after the initial rapid expansion of the SCS, which may explain the relatively late increase in the concentration of this element.

6.2.5. Bulk elemental composition

Major or trace elements present in seawater are either dissolved or absorbed onto particles, which are further removed and deposited into sediments through biotic or abiotic processes. Biotic processes usually involve the uptake of micro- or macronutrients by plankton (mainly phytoplankton), while abiotic processes are either triggered or suppressed by changing redox conditions. These processes will correspondingly produce changing enrichment patterns, which are determined by the individual chemical properties of different elements. In Sections 6.2.1 to 6.2.4, we present a systematic investigation into the elemental geochemistry of Well XK1 in the Xisha Islands. Our samples have suffered a moderate degree of burial diagenesis, which makes them suitable proxies for geochemical study.

Several relationships can be seen between major and trace elements and the previously established stratigraphic framework and sedimentary facies. The coherence between elements and elemental pairs has been summarized in Figs. 3 and 4, respectively. These elements and ratios covary with global and local sea-level changes, though they may also be influenced by changes in redox conditions, salinity, or other parameters regulated by water depth. Our proxies exhibit minima close to the core section boundaries, and throughout lowstand successions. Values begin to increase at transgressive surfaces, and enrichments persist throughout transgressive sequence tracts, with maxima near the maximum flooding surfaces. Values then decline after highstand peaks (Fig. 3). Although associations between certain elemental excursions and sea-level changes have been described and examined by previous investigations, the behaviors and distribution patterns of those elements remain subject to multiple controls. As elemental abundances reflect marine sedimentation types, our geochemical criteria prove to be a suitable method for recognizing sea-level variations. However, it should be noted that some elements exhibit dramatic increases since the Pliocene, when overall water depth shallowed. This trend may reflect the rapid input of continent-derived sediment due to intensive activity of the East Asian Monsoon. However, this interpretation is tentative, and requires further investigation.

6.3. Carbonate platform development and sea level changes in the SCS

Previous research, using methods such as lithostratigraphic, stable isotopic, biostratigraphic, and benthic foraminiferal analyses (Miller et al., 2008; Miller et al., 2011), has shown that ice-volume changes and monsoon strengths have a significant impact on global sea-level fluctuations. The reconstructed eustatic curve provides great insights into relative sea-level variation. Based on a comprehensive combination of lithologic observations, sedimentary facies analyses, thin-section identifications, BIT index excursions, and elemental geochemistry analyses, we demonstrate that reef carbonate growth was initiated during the early phase of the Early Miocene, when the Xisha Block started to be characterized by deep marine depositional environments. In response to the rapid expansion of the SCS, the carbonate platforms of the Xisha Islands expanded. This expansion was characterized by the growth of a higher volume of carbonate, over a wider area, at an elevated growth rate. Beach, reef, and lagoonal facies display intense oscillations in the BIT curve. Although some relatively high values do occur, BIT is still much lower during intervals when reef carbonates were preserved in lagoonal setting with water depths of 20 to 30 m. Overall, this index is characterized by lower values during this interval. Moreover, our inorganic geochemical results vary in phase with the organic geochemical data, with both major and trace element indicators increasing in accordance with their individual chemical properties. During this time period, regional tectonic events, together with eustatic sea level, had a significant effect on relative sea-level variations. From the early Middle Miocene to the late Middle Miocene, global sea level dropped significantly (also observed in the Qiongdongnan Basin), and widespread exposure at low tide imposed stress on many reef flats and atolls. During this phase of exposure and atmospheric weathering, surficial carbonates were reworked and re-deposited as beach-facies sediments. Freshwater infiltration favored certain groups of microorganisms, which exhibited high BIT values (Fig. 3).

At the same time, inorganic geochemistry proxies show a rapid decrease due to shallower water depths. During the subsequent highstand, from the Late Miocene to the Pliocene, when a deeper and more stable marine environment was established, the Xisha carbonate platform grew over the preceding substrate, and produced mature limestone coral reef structures, and fringing lagoons composed of bioclastic sand. Well XK1 is located just inside the lagoonal setting, with greater water depths favoring the survival of marine Crenarchaeota, and depressed values of BIT. Trace elements are highly enriched in the lagoonal system, due to the proliferation of algal organisms, as has been observed in a recent study of mesophotic reefs (Abbey et al., 2013). However, petrographic observation of the core samples shows that organic matter is preserved as discontinuous layers during this interval, which requires a relatively unproductive open oceanic environment, or indicates weak circulation. Therefore, a more restricted topographic configuration of the lagoonal facies is inferred, with a possible depth of ~35–50 m. Conversely, the Pleistocene was characterized by an unstable meteoric-marine diagenetic environment, influenced by high-amplitude global and regional eustatic variations. Reef structures were affected by strong leaching and corrosion processes, resulting in ubiquitous mixing of reef and beach facies. During this interval, BIT became elevated, while assemblages of elements and their ratios are restricted to lower values. With all factors considered, BIT and individual element proxies from Well XK1 prove to be excellent tools for reconstructing sea-level variations in the SCS and the evolution of carbonate platforms since the Early Miocene.

During the Early Miocene, coral reef carbonates started to develop on the rapidly subsiding basement of the Xisha area, which was then isolated from the main continental margin and experienced low fluxes of terrestrial clastic sediment. Later, these Xisha Islands bioherms continued to grow at a relatively high rate, producing alternating lagoon and beach environments. During this interval, the SCS started to subside after an original period of expansion, and subsidence sped up after the Later Miocene. Meanwhile, eustatic sea level remained in a lowstand mode. Based on both tectonic controls and eustatic variations, relative sea level stopped rising and began to fall prior to the late Middle and Upper Miocene. The carbonates in Well XK1 consist of interbedded reef and beach facies, modified by the corrosion and leaching processes that occur

under conditions of meteoric-marine mixing. Afterwards, sea level increased continuously from the Late Miocene to the Pliocene, and atoll reef terraces dominated by lagoon and beach facies expanded. The inner sides of these atolls were exposed to weak corrosion and leaching processes. Overall relative sea level was declining from its previous maximum throughout the Pleistocene, in spite of a few deviations from the general trend. During this sea-level lowstand, most of the carbonate platform represented by Well XK1 was eroded in a freshwater diagenetic environment. Carbonates overlain by reef and beach facies were widely deposited in this sedimentary setting (Fig. 6).

Our inferred overall trend of relative sea-level changes is consistent with eustatic sea-level fluctuations. Interestingly, our proxies are characterized by a common inflection point at a depth of 180 m, which lags slightly behind global sea-level changes, as well as the Pleistocene/Pliocene boundary (216 m), which has been verified by chronostratigraphic studies (Gradstein et al., 2012). Interestingly, the inflection point in BIT and the elemental indicators is synchronous with the initiation of sea-level fall in the Qiongdongnan Basin (Hao et al., 2000). Previous studies have found evidence for increasing subsidence in the northern SCS area after the initial syn-rifting processes, which led to a large-scale rise in relative sea-level (Xie et al., 2014; Zhao et al., 2016). Therefore, regional variations in sea level controlled the development of the Xisha carbonate platforms, to a larger degree than global eustatic factors (Fig. 3). We can conclude that the SCS was not only affected by

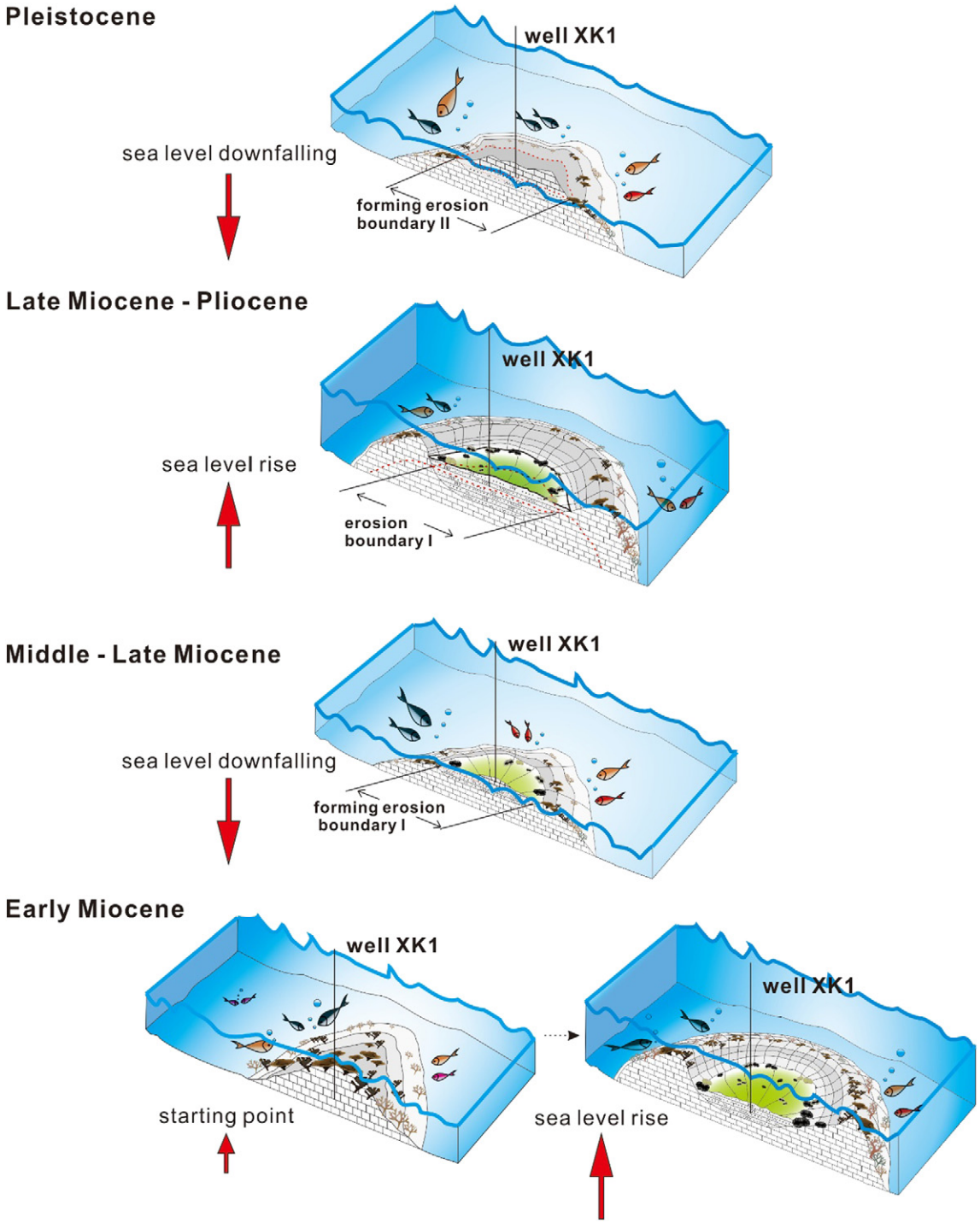

Fig. 6. Carbonate platform evolution in the Xisha Islands. The borehole location is displayed for each time interval. Sea-level fluctuations are denoted by arrows.

global eustatic changes, but was also modified by regional tectonic activity.

7. Conclusions

This study provides a systematic reconstruction of the evolution of the Xisha Islands carbonate platforms, and of sea-level changes in the SCS since the Early Miocene. Our results, which are based on petrographic, biostratigraphic, sedimentological, and elemental and organic geochemical characteristics, indicate that carbonate buildups in the Xisha area reflect a unique pattern of long-term coral reef platform development. We conclude that:

1. BIT, which is derived from GDGTs in the membrane lipids of marine organisms, was examined for the first time in marine carbonates. BIT proves to be an effective index for paleoenvironmental reconstruction, with relatively little influence from diagenetic processes.
2. Classical elemental geochemical analysis was also applied, to examine sea-level variations. Due to our unique study location and the chemistry of the sediments, some elements or related ratios can be used as high-resolution indicators of sea level.
3. Both organic and inorganic geochemical proxies yield SCS sea-level reconstructions that are in good agreement with each other. This strong agreement indicates that a wide variety of proxies need to be considered when reconstructing sea-level at a regional scale.
4. A "four-stage" evolutionary model was reconstructed for the Xisha reef platforms: i) With the rapid opening of the SCS in the Early Miocene, coral reef growth was promoted by increasing water depth, which produced a lagoonal-atoll formation. ii) During the late stage of the Middle Miocene, when sea level dropped significantly, reef structures were exposed to meteoric conditions and deeply eroded. iii) Rising sea level starting in the Late Miocene led to a recurrence of Xisha bioherm platform buildup, culminating in the development of lagoonal facies throughout the Pliocene. iv) During the Pleistocene, sea level oscillated with high frequencies and large amplitudes, and reef structures were frequently exposed to intensive leaching and erosional processes. This process continued until the early Holocene sea level rise.
5. In addition to eustatic sea-level fluctuations, the SCS was also greatly influenced by both vertical and lateral tectonic movements, resulting in regional variations in sea-level. Further detailed investigation of regional tectonism may solve the problem of apparent asynchronization.

Acknowledgments

This study used samples and data provided by CNOOC Ltd.-Zhanjiang. Funding was provided by National Major Science and Technology Project No. 2017ZX05026005-005, and the National Natural Science Foundation of China (project Nos. 41576059, 91128207). Reviewers offered critical comments and suggestions, which greatly improved this work.

Appendix A. Supplementary data

Supplementary data to this article can be found online at http://dx.doi.org/10.1016/j.palaeo.2017.07.006.

References

Abbey, E., Webster, J.M., Braga, J.C., Jacobsen, G.E., Thorogood, G., Thomas, A.L., Camoin, G., Reimer, P.J., Potts, D.C., 2013. Deglacial mesophotic reef demise on the Great Barrier Reef. Palaeogeogr. Palaeoclimatol. Palaeoecol. 392, 473–494.

Arosi, H.A., Wilson, M.E.J., 2015. Diagenesis and fracturing of a large-scale, syntectonic carbonate platform. Sediment. Geol. 326, 109–136.

Bachtel, S.L., Kissling, R.D., Martono, D., Rahardjanto, S.P., Dunn, P.A., MacDonald, B.A., 2004. Seismic stratigraphic evolution of the Miocene-Pliocene Segitiga Platform, East Natuna Sea, Indonesia: the origin, growth, and demise of an isolated carbonate platform. In: Erberli, G.P., Masaferro, J.L., Sarg, J.F. (Eds.), Seismic Imaging of Carbonate Reservoirs and Systems. American Association of Petroleum Geologists, Tulsa, Oklahoma, pp. 309–328.

Barckhausen, U., Roeser, H.A., 2004. Seafloor spreading anomalies in the South China Sea revisited. In: Clift, P.D., Wang, P.X., Kuhnt, W., Hall, R., Tada, R. (Eds.), Continent-Ocean Interactions Within East Asian Marginal Seas. American Geophysical Union, Washington, D. C., pp. 121–125.

Beck, J.W., Edwards, R.L., Ito, E., Taylor, F.W., Recy, J., Rougerie, F., Joannot, P., Henin, C., 1992. Sea-surface temperature from coral skeletal strontium/calcium ratios. Science 257, 644–647.

Bertrand, P., Pedersen, T.F., Martinez, P., Calvert, S., Shimmield, G., 2000. Sea level impact on nutrient cycling in coastal upwelling areas during deglaciation: evidence from nitrogen isotopes. Glob. Biogeochem. Cycles 14, 341–356.

Broecker, W.S., Thurber, D.L., Goddard, J., Ku, T.L., Matthews, R.K., Mesolella, K.J., 1968. Milankovitch hypothesis supported by precise dating of coral reefs and deep-sea sediments. Science 159, 297–300.

Cantalejo, B., Pickering, K.T., 2014. Climate forcing of fine-grained deep-marine systems in an active tectonic setting: Middle Eocene, Ainsa Basin, Spanish Pyrenees. Palaeogeogr. Palaeoclimatol. Palaeoecol. 410, 351–371.

Cappellen, P.V., Ingall, E.D., 1994. Benthic phosphorus regeneration, net primary production, and ocean anoxia: a model of the coupled marine biogeochemical cycles of carbon and phosphorus. Paleoceanography 9, 677–692.

Chappell, J., 1983. Evidence for smoothly falling sea level relative to north Queensland, Australia, during the past 6000 yr. Nature 302, 406–408.

Clift, P.D., Lin, J., 2001. Patterns of extension and magmatism along the continent-ocean boundary, South China margin. Geol. Soc. Lond., Spec. Publ. 187, 489–510.

Dan, B., 2005. A genetic classification of carbonate platforms based on their basinal and tectonic settings in the Cenozoic. Sediment. Geol. 175, 49–72.

Dean, W.E., Piper, D.Z., Peterson, L.C., 1999. Molybdenum accumulation in Cariaco basin sediment over the past 24 k.y.: a record of water-column anoxia and climate. Geology 27, 507–510.

Degens, E.T., Ross, D.A., 1974. Black Sea—Geology, Chemistry, and Biology. American Association of Petroleum Geologists, Talsa, Oklahoma.

Derry, L.A., Kaufman, A.J., Jacobsen, S.B., 1992. Sedimentary cycling and environmental change in the Late Proterozoic: evidence from stable and radiogenic isotopes. Geochim. Cosmochim. Acta 56, 1317–1329.

Edinger, E.N., Burr, G.S., Pandolfi, J.M., Ortiz, J.C., 2007. Age accuracy and resolution of Quaternary corals used as proxies for sea level. Earth Planet. Sci. Lett. 253, 37–49.

Elderfield, H., 1990. Tracers of ocean paleoproductivity and paleochemistry: an introduction. Paleoceanography 5, 711–717.

Erlich, R.N., Barrett, S.F., Guo, B.J., Erlich, R.N., Guo, B.J., 1990. Seismic and geologic characteristics of drowning events on carbonate platforms. Am. Assoc. Pet. Geol. Bull. 74, 1523–1537.

Erlich, R.N., L. Jr., A.P., Hyare, S., 1993. Response of carbonate platform margins to drowning: evidence of environmental collapse. Am. Assoc. Petr. Geol. Mem. 57, 241–266.

Fallon, S.J., White, J.C., Mcculloch, M.T., 2002. Porites corals as recorders of mining and environmental impacts: Misima Island, Papua New Guinea. Geochim. Cosmochim. Acta 66, 45–62.

Filippelli, G.M., Delaney, M.L., 1996. Phosphorus geochemistry of equatorial Pacific sediments. Geochim. Cosmochim. Acta 60, 1479–1495.

Flügel, E., Munnecke, A., 2004. Microfacies of Carbonate Rocks: Analysis, Interpretation and Application. Springer.

Fournier, F., Borgomano, J., Montaggioni, L.F., 2004. Paleoenvironments and high-frequency cyclicity from Cenozoic South-East Asian shallow-water carbonates: a case study from the Oligo–Miocene buildups of Malampaya (Offshore Palawan, Philippines). Mar. Pet. Geol. 21, 1–21.

Fournier, F., Borgomano, J., Montaggioni, L.F., 2005. Development patterns and controlling factors of Tertiary carbonate buildups: insights from high-resolution 3D seismic and well data in the Malampaya gas field (Offshore Palawan, Philippines). Sediment. Geol. 175, 189–215.

Francois, R., 1988. A study on the regulation of the concentrations of some trace metals (Rb, Sr, Zn, Pb, Cu, V, Cr, Ni, Mn and Mo) in Saanich Inlet Sediments, British Columbia, Canada. Mar. Geol. 83, 285–308.

Fulthorpe, C.S., Schlanger, S.O., 1989. Paleo-oceanographic and tectonic settings of early Miocene reefs and associated carbonates of offshore southeast Asia. AAPG Bull. Am. Assoc. Pet. Geol. 73, 729–756.

Gentsch, A., Schützbosbach, S., 2000. Widespread occurrence of structurally diverse tetraether membrane lipids: evidence for the ubiquitous presence of low-temperature relatives of hyperthermophiles. Proc. Natl. Acad. Sci. 97, 14421–14426.

Gradstein, F.M., Ogg, J.G., Schmitz, M., 2012. Erdgeschichte. The Geologic Time Scale 2012. vol. 2. Elsevier Science & Technology.

Hao, Y.C., Chen, P.F., Wan, X., Dong, J., 2000. Late Tertiary sequence stratigraphy and sea level changes in Yinggehai Qiongdongnan Basin. Geoscience 14, 237–245 (in Chinese with English abstract).

Haq, B.U., 1988. Mesozoic and Cenozoic Chronostratigraphy and Cycles of Sea-level Changes: An Integrated Approach. In: Wilgus, C.K., Hastings, B.S., Posamentier, H., Wagoner, J.V., Ross, C.A., Kendall, C.G.S.C. (Eds.), Spec. Publ. Soc. Econ. Paleontol. Mineral. No. 42, 71–108.

Holloway, N.H., 1982. North Palawan Block, Philippines—its relation to Asian mainland and role in evolution of South China Sea. Am. Assoc. Pet. Geol. Bull. 66, 1355–1383.

Hopmans, E.C., Schouten, S., Pancost, R.D., Meer, M.T.J.V.D., Damsté, J.S.S., 2000. Analysis of intact tetraether lipids in archaeal cell material and sediments by high performance liquid chromatography/atmospheric pressure chemical ionization mass spectrometry. Rapid Commun. Mass Spectrom. 14, 585–589.

Hopmans, E.C., Weijers, J.W.H., Schefuß, E., Herfort, L., Sinninghe Damsté, J.S., Schouten, S., 2004. A novel proxy for terrestrial organic matter in sediments based on branched and isoprenoid tetraether lipids. Earth Planet. Sci. Lett. 224, 107–116.

Huguet, C., Hopmans, E.C., Febo-Ayala, W., Thompson, D.H., Damsté, J.S.S., Schouten, S., 2006. An improved method to determine the absolute abundance of glycerol dibiphytanyl glycerol tetraether lipids. Org. Geochem. 37, 1036–1041.
Huguet, C., Lange, G.J.D., Gustafsson, Ö., Middelburg, J.J., Damsté, J.S.S., Schouten, S., 2008. Selective preservation of soil organic matter in oxidized marine sediments (Madeira Abyssal Plain). Geochim. Cosmochim. Acta 72, 6061–6068.
Huguet, C., Kim, J.H., Lange, G.J.D., Damsté, J.S.S., Schouten, S., 2009. Effects of long term oxic degradation on the U37K′, TEX86 and BIT organic proxies. Org. Geochem. 40, 1188–1194.
Hutchison, C.S., 2004. Marginal basin evolution: the southern South China Sea. Mar. Pet. Geol. 21, 1129–1148.
Jacobs, L., Emerson, S., Huested, S.S., 1987. Trace metal geochemistry in the Cariaco Trench. Deep Sea Res. Part A 34, 965–981.
Jarvis, I., 2001. Geochemistry of pelagic and hemipelagic carbonates: criteria for identifying systems tracts and sea-level change. J. Geol. Soc. 158, 685–696.
Johnston, P., 2007. The effect of spatially non-uniform water loads on prediction of sea-level change. Geophys. J. Int. 114, 615–634.
Kaufman, A.J., Knoll, A.H., 1995. Neoproterozoic variations in the C-isotopic composition of seawater: stratigraphic and biogeochemical implications. Precambrian Res. 73, 27–49.
Kaufman, A.J., Jacobsen, S.B., Knoll, A.H., 1993. The Vendian record of Sr and C isotopic variations in seawater: implications for tectonics and paleoclimate. Earth Planet. Sci. Lett. 120, 409–430.
Kaufmann, G., Lambeck, K., 2000. Mantle dynamics, postglacial rebound and the radial viscosity profile. Phys. Earth Planet. Inter. 121, 301–324.
Kendall, C.G.S.C., Schlager, W., 1981. Carbonates and relative changes in sea level. Mar. Geol. 44, 181–212.
Kinsey, D.W., Davies, P.J., 1979. Effects of elevated nitrogen and phosphorus on coral reef growth. Limnol. Oceanogr. 24 (5), 935–940.
Knauer, G.A., Martin, J.H., 1983. Trace elements and primary production: problems, effects and solutions. In: Wong, C.S., Boyle, E., Bruland, K.W., Burton, J.D., Goldberg, E.D. (Eds.), Trace Metals in Sea Water. Springer, U. S. A., pp. 825–840.
Lambeck, K., Chappell, J., 2001. Sea level change through the last glacial cycle. Science 292, 679–686.
Langmuir, D., 1978. Uranium solution-mineral equilibria at low temperatures with applications to sedimentary ore deposits. Geochim. Cosmochim. Acta 42, 547–569.
Lisiecki, L.E., Raymo, M.E., 2005. Pliocene-Pleistocene stack of 57 globally distributed benthic $\delta^{18}O$ records. Paleoceanography 20, 1–16.
Liu, J., Ye, Z., Han, C., Liu, X., Qu, G., 1997. Meteoric diagenesis in Pleistocene reef limestones of Xisha Islands, China. J. Asian Earth Sci. 15, 465–476.
Longman, M.W., Siemers, C.T., 1992. Carbonate Rocks and Reservoirs of Indonesia: Core Workshop Introduction and Overview. Indonesian Petroleum Association.
Lowenstein, T.K., Timofeeff, M.N., Brennan, S.T., Hardie, L.A., Demicco, R.V., 2001. Oscillations in Phanerozoic seawater chemistry: evidence from fluid inclusions. Science 294, 1086–1088.
Lü, C., Wu, S., Yao, Y., Fulthorpe, C.S., 2013. Development and controlling factors of Miocene carbonate platform in the Nam Con Son Basin, southwestern South China Sea. Mar. Pet. Geol. 45, 55–68.
Lüdmann, T., Kalvelage, C., Betzler, C., 2013. The Maldives, a giant isolated carbonate platform dominated by bottom currents. Mar. Pet. Geol. 43, 326–340.
Lydie, H., Stefan, S., Boon, J.P., Martijn, W., Marianne, B., Weijers, J.W.H., Sinninghe, D.J.S., 2006. Characterization of transport and deposition of terrestrial organic matter in the Southern North Sea using the BIT index. Limnol. Oceanogr. 51, 2196–2205.
Ma, Y., Wu, S., Lv, F., Dong, D., Sun, Q., Lu, Y., Gu, M., 2011. Seismic characteristics and development of the Xisha carbonate platforms, northern margin of the South China Sea. J. Asian Earth Sci. 40, 770–783.
Mangini, A., Eisenhauer, A., Walter, P., 1990. The response of manganese in the ocean to the climatic cycles in the Quaternary. Paleoceanography 5, 811–821.
Masao, N., Kurt, L., 1987. Glacial rebound and relative sea-level variations: a new appraisal. Geophys. J. Int. 90, 171–224.
Meyers, W.J., 1974. Carbonate cement stratigraphy of the Lake Valley Formation (Mississippian) Sacramento Mountains, New Mexico. J. Sediment. Res. 837–861.
Miller, K.G., Browning, J.V., Aubry, M.P., Wade, B.S., Katz, M.E., Kulpecz, A.A., Wright, J.D., 2008. Eocene-Oligocene global climate and sea-level changes: St. Stephens Quarry, Alabama. Geol. Soc. Am. Bull. 120, 34–53.
Miller, K.G., Mountain, G.S., Wright, J.D., Browning, J.V., 2011. A 180-million-year record of sea level and ice volume variations from continental margin and deep-sea isotopic records. Oceanography 24, 40–53.
Moss, S.J., Chambers, J.L.C., 1999. Tertiary facies architecture in the Kutai Basin, Kalimantan, Indonesia. J. Asian Earth Sci. 17, 157–181.
Murray, R.W., Leinen, M., 1993. Chemical transport to the seafloor of the equatorial Pacific Ocean across a latitudinal transect at 135°W: tracking sedimentary major, trace, and rare earth element fluxes at the Equator and the Intertropical Convergence Zone. Geochim. Cosmochim. Acta 57, 4141–4163.
Nakajima, T., Kikkawa, K., Ikehara, K., Katayama, H., Kikawa, E., Joshima, M., Seto, K., 1996. Marine sediments and late Quaternary stratigraphy in the southeastern part of the Japan Sea. Concerning the timing of dark layer deposition. J. Geol. Soc. Jpn. 102, 125–138.
Pattan, J.N., Pearce, N.J.G., 2009. Bottom water oxygenation history in southeastern Arabian Sea during the past 140 ka: results from redox-sensitive elements. Palaeogeogr. Palaeoclimatol. Palaeoecol. 280, 396–405.
Paumard, V., Zuckmeyer, E., Boichard, R., Jorry, S.J., Bourget, J., Borgomano, J., Maurin, T., Ferry, J.N., 2016. Evolution of Late Oligocene-Early Miocene attached and isolated carbonate platforms in a volcanic ridge context (Maldives type), Yadana field, offshore Myanmar. Mar. Pet. Geol. 361–387.
Purdy, E.G., 1974. Karst-determined facies patterns in British Honduras: Holocene carbonate sedimentation model. Am. Assoc. Pet. Geol. Bull. 58, 825–855.
Qiao, P.J., Zhu, W.L., Shao, L., Zhang, D.J., Cheng, X.R., Song, Y.M., 2015. Carbonate stable isotope stratigraphy of well Xike-1, Xisha Islands. Earth Sci. J. China Univ. Geosci. 40, 725–732 (in Chinese with English abstract).
Redfield, A.C., 1958. The biological control of chemical factors in the environment. Sci. Prog. 46, 150–170.
Rougerie, F., Fagerstrom, J., 1994. Cretaceous history of Pacific Basin guyot reefs: a reappraisal based on geothermal endo-upwelling. Palaeogeogr. Palaeoclimatol. Palaeoecol. 112, 239–260.
Sales, A.O., Jacobsen, E.C., Morado, A.A., Benavidez, J.J., Navarro, F.A., Lim, A.E., 1997. The petroleum potential of deep-water northwest Palawan Block GSEC 66. J. Asian Earth Sci. 15, 217–240.
Saltzman, M.R., 2005. Phosphorus, nitrogen, and the redox evolution of the Paleozoic oceans. Geology 33, 573–576.
Schmitz, B., 1987. Barium, equatorial high productivity, and the northward wandering of the Indian continent. Paleoceanography 2, 63–77.
Schneider, R.R., Price, B., Müller, P.J., Kroon, D., Alexer, I., 1997. Monsoon related variations in Zaire (Congo) sediment load and influence of fluvial silicate supply on marine productivity in the east equatorial Atlantic during the last 200,000 years. Paleoceanography 12, 463–482.
Schouten, S., Hopmans, E.C., Schefuß, E., Damsté, J.S.S., 2002. Distributional variations in marine crenarchaeotal membrane lipids: a new tool for reconstructing ancient sea water temperatures? Earth Planet. Sci. Lett. 204, 265–274.
Schouten, S., Hopmans, E.C., Baas, M., Boumann, H., Standfest, S., Könneke, M., Stahl, D.A., 2008. Intact membrane lipids of "*Candidatus Nitrosopumilus maritimus*," a cultivated representative of the Cosmopolitan Mesophilic Group I Crenarchaeota. Appl. Environ. Microbiol. 74, 2433–2440.
Schouten, S., Hopmans, E.C., Damsté, J.S.S., 2013. The organic geochemistry of glycerol dialkyl glycerol tetraether lipids: a review. Org. Geochem. 54, 19–61.
Shao, L., Li, Q., Zhu, W., Zhang, D., Qiao, P., Liu, X., You, L., Cui, Y., Dong, X., 2017. Neogene carbonate platform development in the NW South China Sea: Litho-, bio- and chemo-stratigraphic evidence. Mar. Geol. 385, 233–243.
Shi, X., Zhou, D., Qiu, X., Zhang, Y., 2002. Thermal and rheological structures of the Xisha Trough, South China Sea. Tectonophysics 351, 285–300.
Sinninghe Damsté, J.S., Hopmans, E.C., Pancost, R.D., Schouten, S., Geenevasen, J.A.J., 2000. Newly discovered non-isoprenoid glycerol dialkylglycerol tetraether lipids in sediments. Chem. Commun. 17, 1683–1684.
Sinninghe Damsté, J.S., Schouten, S., Hopmans, E.C., van Duin, A.C., Geenevasen, J.A., 2002. Crenarchaeol: the characteristic glycerol dibiphytanyl glycerol tetraether membrane lipid of cosmopolitan pelagic Crenarchaeota. J. Lipid Res. 43, 1641–1651.
Sinninghe Damsté, J.S., Ossebaar, J., Abbas, B., Schouten, S., Verschuren, D., 2009. Fluxes and distribution of tetraether lipids in an equatorial African lake: constraints on the application of the TEX 86 palaeothermometer and BIT index in lacustrine settings. Geochim. Cosmochim. Acta 73, 4232–4249.
Sluijs, A., Brinkhuis, H., Crouch, E.M., John, C.M., Handley, L., Munsterman, D., Bohaty, S.M., Zachos, J.C., Reichart, G.J., Schouten, S., 2008. Eustatic variations during the Paleocene-Eocene greenhouse world. Paleoceanography 23, 101–106.
Steuer, S., Franke, D., Meresse, F., Savva, D., Pubellier, M., Auxietre, J.L., Aurelio, M., 2013. Time constraints on the evolution of southern Palawan Island, Philippines from onshore and offshore correlation of Miocene limestones. J. Asian Earth Sci. 76, 412–427.
Stüben, D., Kramar, U., Berner, Z., Stinnesbeck, W., Keller, G., Adatte, T., 2002. Trace elements, stable isotopes, and clay mineralogy of the Elles II K–T boundary section in Tunisia: indications for sea level fluctuations and primary productivity. Palaeogeogr. Palaeoclimatol. Palaeoecol. 178, 321–345.
Taylor, B., Hayes, D.E., 1983. Origin and history of the South China Sea basin. In: Hayes, D.E. (Ed.), The Tectonic and Geologic Evolution of Southeast Asian Seas and Islands: Part 2. American Geophysical Union, Washington D. C., pp. 23–56.
Taylor, S.R., McLennan, S.M., 1995. The geochemical evolution of the continental crust. Rev. Geophys. 33, 241–265.
Umbgrove, J.H.F., 1947. Coral reefs of the East Indies. Geol. Soc. Am. Bull. 58, 729–778.
Van, S.W.A., Kominz, M.A., Miller, K.G., Browning, J.V., 2004. Late Cretaceous and Cenozoic sea-level estimates: backstripping analysis of borehole data, onshore New Jersey. Basin Res. 16, 451–465.
Walsh, E.M., Ingalls, A.E., Keil, R.G., 2008. Sources and transport of terrestrial organic matter in Vancouver Island fjords and the Vancouver-Washington Margin: a multiproxy approach using d13Corg, lignin phenols, and the ether lipid BIT index. Limnol. Oceanogr. 53, 1054–1063.
Weijers, J.W.H., Schouten, S., Hopmans, E.C., Geenevasen, J.A.J., David, O.R.P., Coleman, J.M., Pancost, R.D., Damsté, J.S.S., 2006. Membrane lipids of mesophilic anaerobic bacteria thriving in peats have typical archaeal traits. Environ. Microbiol. 8, 648–657.
Wignall, P.B., Twitchett, R.J., 1996. Oceanic anoxia and the end Permian mass extinction. Science 272, 1155–1158.
Wilson, M.E.J., 2002. Cenozoic carbonates in Southeast Asia: implications for equatorial carbonate development. Sediment. Geol. 147, 295–428.
Wood, R., 1993. Nutrients, predation and the history of reef-building. PALAIOS 8, 526–543.
Wu, S., Yang, Z., Wang, D., Lü, F., Lüdmann, T., Fulthorpe, C., Wang, B., 2014. Architecture, development and geological control of the Xisha carbonate platforms, northwestern South China Sea. Mar. Geol. 350, 71–83.
Wu, S., Zhang, X., Yang, Z., Wu, T., Gao, J., Wang, D., 2016. Spatial and temporal evolution of Cenozoic carbonate platforms on the continental margins of the South China Sea: response to opening of the ocean basin. Interpretation 4, 1–19.

Wyndham, T., Mcculloch, M., Fallon, S., Alibert, C., 2004. High-resolution coral records of rare earth elements in coastal seawater: biogeochemical cycling and a new environmental proxy 3. Geochim. Cosmochim. Acta 68, 2067–2080.

Xi, W., Fu, D.J., Yan, X.W., Zhu, Y.J., Zhao, G.C., Xi, L.Y., Han, C.Y., 2005. Constraints on biogenetic reef formation during evolution of the South China Sea and exploration potential analysis. Earth Sci. Front. 12, 245–252.

Xie, H., Zhou, D., Li, Y., Pang, X., Li, P., Chen, G., Li, F., Cao, J., 2014. Cenozoic tectonic subsidence in deepwater sags in the Pearl River Mouth Basin, northern South China Sea. Tectonophysics 615–616, 182–198.

Zhao, Z., Sun, Z., Sun, L., Wang, Z., Sun, Z., 2016. Cenozoic tectonic subsidence in the Qiongdongnan Basin, Northern South China Sea. Basin Res. 1–20.